

Extracting order within disorder in disordered materials by high-energy X-ray diffraction

The structure of disordered materials is not highly disorganized: these materials have some degree of intermediate-range ordering [1]. The advent of third-generation synchrotron radiation sources, which can generate high-flux, high-energy X-rays, and the development of advanced instruments allow probing atomic arrangements in disordered materials with high real-space resolution. A combination of quantum beam (X-ray and neutron) diffraction, theoretical simulations (such as density functional theory (DFT) and molecular dynamics (MD)), and data-driven structural modeling (such as reverse Monte Carlo (RMC) modeling [2]) facilitates ordering within disorder in disordered materials. In this article, a dedicated high-energy X-ray diffractometer installed at SPring-8 BL04B2 [3] is introduced and, recent studies on probing the intermediate ordering in disordered materials are reviewed. In particular, recently discovered extraordinarily ordered oxide glasses and liquids are addressed to discuss the relationship between diffraction peaks and intermediate-range ordering in disordered materials.

High-energy X-ray diffractometer

A dedicated X-ray pair distribution function (PDF) diffractometer for disordered materials was developed at SPring-8 BL04B2 in 1999. The light source of BL04B2 is a bending magnet with a critical energy of 28.9 keV; additionally, the single-bounce bent Si 220 and Si 511 crystals with a Bragg angle fixed at 3°

provide 61.7 and 113.3 keV X-rays, respectively. The beamline details are described in a previous study [3]. The advantages of our dedicated diffractometer are the extremely low background and high reliability of the diffraction data, which are important factors for obtaining accurate PDF data.

A dedicated diffractometer for disordered materials has been operating for over 20 years at BL04B2. The first- and second-generation detectors were intrinsic germanium (Ge) and triple-cadmium telluride (CdTe), respectively. The advantage of a Ge detector is its supersensitivity, which is important in the high-diffraction-angle region, because the diffraction intensity is weak in the high-scattering-vector Q (high diffraction angle) region owing

to the decay of the Q -dependent atomic form factors. The efficiency of the Ge detector is comparable to that of the CdTe detector at 61.7 keV; however, it is 1.8 times higher at 113.3 keV. In addition, the size of the Ge detector element is much larger than that of CdTe. Previous studies confirmed that approximately twice the gain is obtained with a Ge detector compared with a CdTe detector at 61.7 keV, thus suggesting that an approximately four-fold higher gain is achieved at 113.3 keV. Another advantage of a semiconductor detector is its high energy resolution for discriminating fluorescence from the sample and the signal of the higher harmonic reflections of the monochromator crystal. The energy resolution (FWHM) of CdTe detectors is better than 3.1 keV,

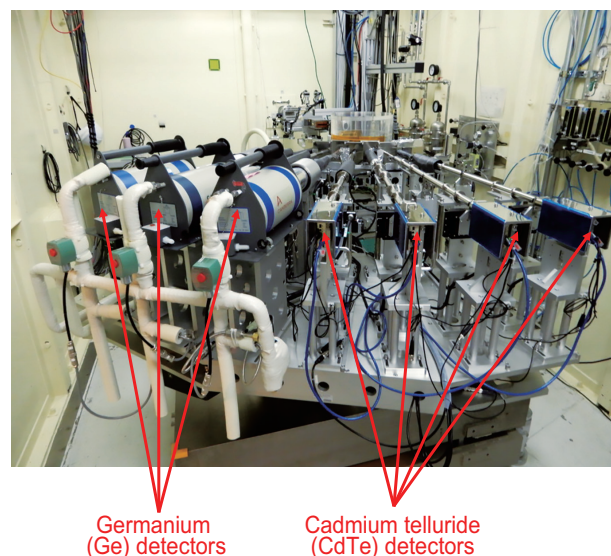


Fig. 1. High-energy X-ray PDF diffractometer installed BL04B2 [3].

whereas that of Ge detectors is better than 1.0 keV. The primary disadvantage of the Ge detector is the necessity to replenish liquid nitrogen, which interrupts the measurement. On the other hand, the advantage of a CdTe detector is its small size, which renders it suitable for covering low-diffraction-angle regions where space is limited. Another advantage of the CdTe detector is that it uses a Peltier device cooling system owing to its small detector elements. In a recent upgrade, four CdTe detectors were installed for low-diffraction-angle regions and three Ge detectors with an automated liquid nitrogen filling system were installed for high-diffraction-angle regions. The typical setup of the upgraded diffractometer is shown in Fig. 1.

Analysis of diffraction data by structure modeling techniques

Important quantitative structural information on short- and intermediate-range orders in glasses can be obtained from the atom distribution functions derived using X-ray and neutron diffraction. Modeling techniques are necessary to obtain more realistic and useful structural information from diffraction data, particularly for intermediate-range orders. RMC modeling allows for a quantitative fit of the experimental data without the use of potential functions. Compared with MD and/or standard Monte Carlo simulation techniques, RMC is particularly useful for the study of multicomponent glasses, for which the determination of interatomic potential functions for chemical bonding is difficult. The combination of RMC modeling and MD simulations has become popular for obtaining more reliable structural models [2].

Structure of oxide glasses and liquids

Oxide glasses, such as window glass, fiber glass, and optical glass, are essential daily-use materials. The most conventional glass formation

method is melt quenching, in which the glass-forming ability (GFA) is governed by the viscosity of a high-temperature melt. In the last century, Angell proposed the concept of “fragility” based on the temperature-dependent behavior of viscosity to understand the relationship between viscosity and GFA [4]. The basic concept underlying glass formation is a corner-sharing tetrahedral motif proposed by Zachariasen in 1932 [5]. Fifteen years later, Sun classified single-component oxides as glass formers, glass modifiers, and intermediates [6]. Silica (SiO_2) is a prototypical glass former in which the silicon–oxygen coordination number is four, and the glass network is formed by corner-sharing oxygen atoms. In alkali and alkali earth oxides are typical glass modifiers; they cannot solely form glass but rather modify the network formed by a network former by breaking the silicon–oxygen bonds in the network and/or occupying cavities.

Densified silica glass

Figure 2(a) shows the *in situ* neutron structure $S(Q)$ of silica glass under high pressure [7]. The first sharp diffraction peak (FSDP) and

principal peak (PP) were observed in the ambient pressure data (black curve) at Q of approximately 1.5 and 3 \AA^{-1} , respectively. The formation of the FSDP was owing to atomic ordering along the cavities by corner-sharing SiO_4 tetrahedra. The origin of the second PP appeared to be a type of orientational correlation among the oxygen atoms occupying the corners of the tetrahedra, thus suggesting that the PP reflects the packing of oxygen atoms. Upon the application of pressure at room temperature, the FSDP shifted to a high Q and diminishes. By contrast, the PP became very sharp (see Fig. 2(a)), which is associated with a cavity volume reduction. This sharp PP is a signature of orientational correlations formed by oxygen atoms under high pressure.

Figure 2(b) shows the X-ray total structure factors $S(Q)$ of the densified silica glasses obtained by hot compression. These data were not *in situ* diffraction data; however, the FSDP was the sharpest in the sample recovered at 1200 °C/7.7 GPa. This behavior is very different from the *in situ* neutron diffraction data shown in Fig. 2(a). Thus, 1200 °C/7.7 GPa glass was demonstrated as the most ordered silica glass in the world.

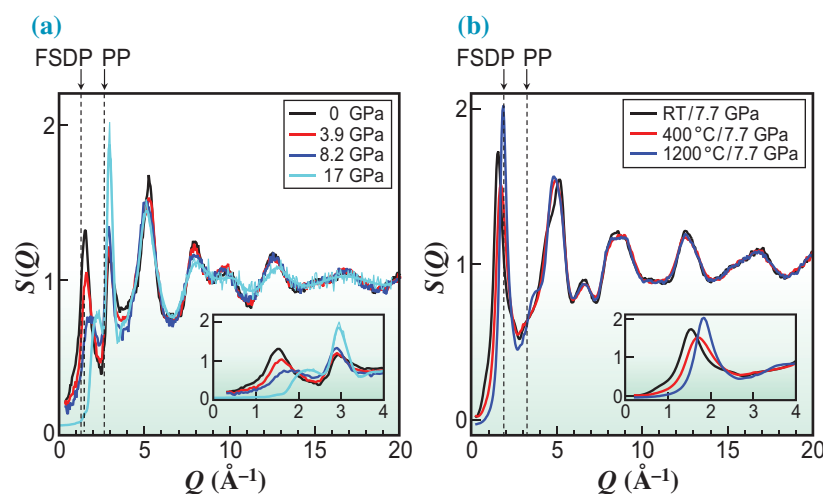


Fig. 2. (a) *In situ* neutron $S(Q)$ of silica glass under high pressure and room temperature [7]. (b) X-ray structure factor $S(Q)$ of densified silica glass recovered at high temperature and high pressure [8].

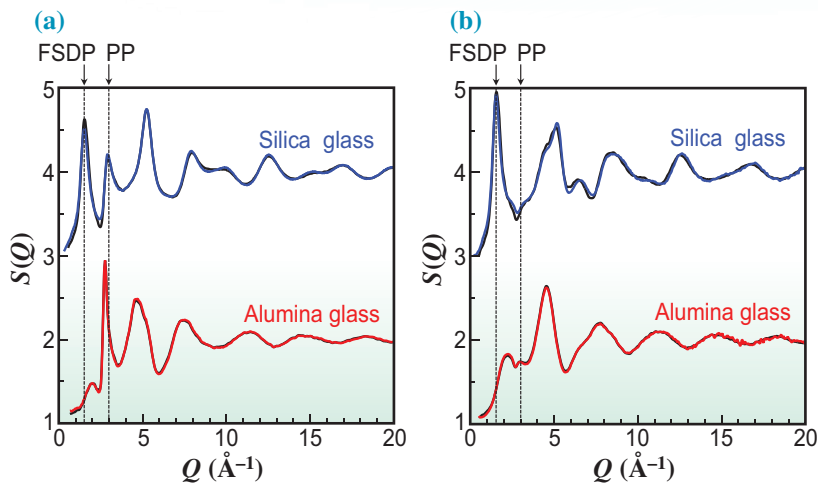


Fig. 3. (a) Neutron and (b) X-ray total structure factors $S(Q)$ of silica and alumina glasses [9]. Blue and red curves: experimental data, black curves: MD-RMC model.

Intermediate alumina glass

Silica is a good glass former, as mentioned above, whereas alumina (Al_2O_3) is not a glass former and is classified as an intermediate according to Sun [6]. Alumina glass cannot be formed using conventional melt-quenching techniques. However, Hashimoto *et al.* recently reported that amorphous alumina synthesized by the anodization of aluminum metal exhibits a glass transition [9]. Figures 3(a) and 3(b) show the neutron and X-ray total structure factors $S(Q)$, respectively, of the silica and alumina glasses. Silica glass exhibited a distinct FSDP owing to its high glass-forming ability. By contrast, alumina glass exhibited an extraordinarily sharp PP in the neutron $S(Q)$ data, similar to the *in situ* high-pressure data of silica glass shown in Fig. 2(a), thus suggesting that the packing density of oxygen atoms is very high in alumina glass. Figure 4 illustrates the atomic arrangement of the alumina glass in a stick representation (a) and cavity visualization (b), where the lattice (crystal)-like atomic arrangement formed by edge-sharing of the AlO_n polyhedra is highlighted by black dotted lines. In addition, numerous sparser regions formed by

the tetrahedral corner-sharing motif were observed (Fig. 4(a)). The cavity volume ratio of alumina glass was 4.5%, which is comparable to those of densified silica glasses recovered at $1200^\circ\text{C}/7.7\text{ GPa}$. Further, the average Al–O coordination number was 4.7, which is much higher than that in silica glass (4), and the formation of AlO_4 , AlO_5 , and AlO_6 was confirmed. This variation in Al–O coordination is the reason for the formation of edge-sharing Al–O polyhedra, which can disturb the evolution of the intermediate-range ordering detected as an FSDP.

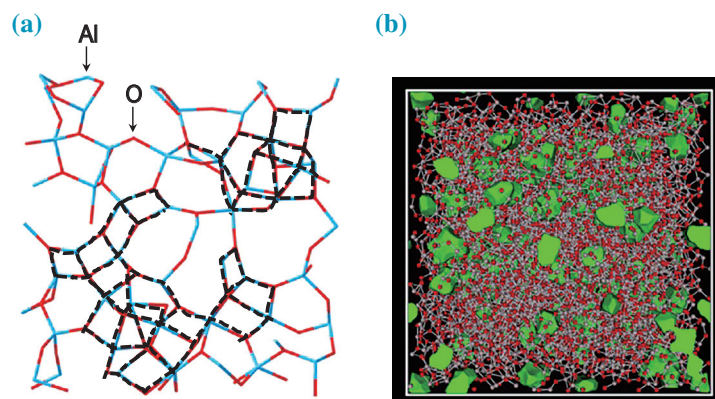


Fig. 4. Atomic arrangements of alumina glass in: (a) stick representation and (b) with cavity visualization [9].

Levitated erbia liquid

Erbia (Er_2O_3) is a nonglass-forming material with an extremely high melting point ($T_m = 2430^\circ\text{C}$). To perform diffraction measurements of such high-temperature liquids, several containerless techniques that enable holding a liquid droplet without a container have been developed [2]. A previous study employed an aerodynamic levitation technique for X-ray measurements, in which a sample is levitated using dry air from a conical nozzle.

Figure 5 shows the X-ray structure factors $S(Q)$ of the erbia liquid (2650°C) [10] (a) and zirconia (ZrO_2) liquid (2800°C) [11] (b), together with those obtained using several simulation techniques. No FSDP were observed in either dataset because they are nonglass-forming materials. However, they exhibited a PP at a Q of approximately 2 \AA^{-1} . The FWHMs of PP for the zirconia and erbia liquids were 0.7669 and 0.4299, respectively. In the case of zirconia liquid, the RMC-DF/MD model of 501 particles (magenta curve) reproduced the experimental data. However, the RMC-MD model of 5000 particles (red curve) was required to reproduce the extraordinarily sharp PP of the erbia liquid. As a benchmark, the number of particles in the standard RMC approach was reduced, and

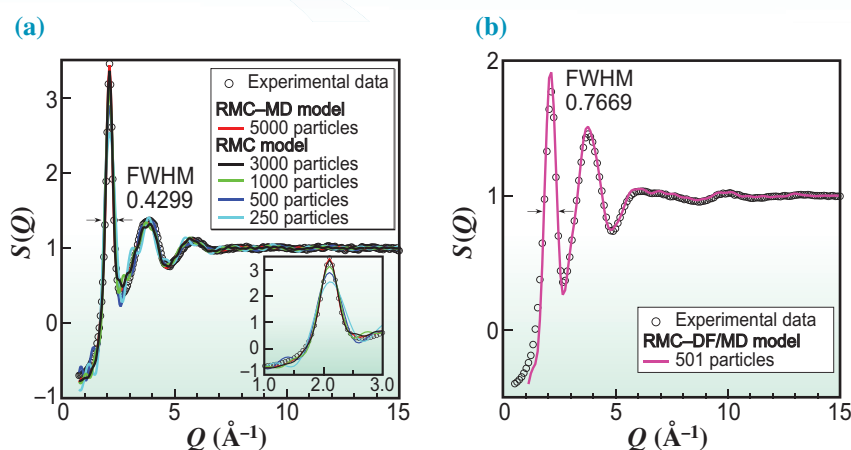


Fig. 5. X-ray structure factors $S(Q)$ of: (a) erbium liquid (2650°C) [10] and (b) zirconia liquid (2800°C) [11], along with those obtained by RMC-MD, RMC, and RMC-DF/MD modeling.

500 particles (blue) were confirmed to be insufficient for reproducing such an extraordinarily sharp PP.

The cation–oxygen coordination number was approximately 6 for both liquids, which is extremely larger than 3.9 for silica SiO_2 liquid (2100°C) and 4.4 for alumina liquid (2127°C). Moreover, the oxygen–cation coordination number was 3.0 for zirconia liquid and 4.1 for erbium liquid, thus suggesting that a large fraction of an OEr_4 tetracluster, which cannot be observed in other liquids, was observed.

Figure 6 illustrates the atomic arrangement of the erbium liquid in the stick representation. Evidently,

an extraordinarily densely packed atomic arrangement, as that found in alumina glass, was observed; however, a sparse region, as that observed in alumina glass, was not observed. This extraordinarily densely packed atomic arrangement, highlighted by the dotted lines, was formed by the edge-sharing ErO_n polydra associated with the formation of OEr_4 tetraclusters and is the origin of the extremely low glass-forming ability and extraordinarily sharp PP.

We review several unusual oxide glasses and liquid structures with respect to. Their structures are significantly different from those of conventional oxide glasses and

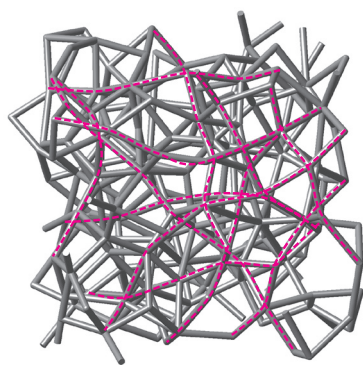


Fig. 6. Atomic arrangement of erbium liquid in stick representation [10].

liquids. The characteristic features of these glasses and liquids are variations in the polyhedra in terms of coordination number and polyhedral connections (corner, edge, and face).

In this article, the high-energy X-ray PDF diffractometer was briefly introduced for disordered materials developed at SPring-8 BL04B2. Combining quantum beam measurements and advanced simulations is a promising method for extracting the hidden order in disordered materials. The results of the advanced analysis can help to forge a new path or designing novel functional disordered materials.

Shinji Kohara^{a,b}

^aNational Institute for Materials Science

^bTokyo University of Science

Email: KOHARA.Shinji@nims.go.jp

References

- [1] P. S. Salmon: *Nat. Mater.* **1** (2002) 87.
- [2] S. Kohara and L. Pusztai: "Atomistic Simulation of Glasses," Ed. by J. Du and A. N. Cormack, Wiley-American Ceramic Society, Hoboken p.60 (2022).
- [3] K. Ohara *et al.*: *J. Phys.: Condens. Matter* **33** (2021) 383001.
- [4] C. A. Angell: *Science* **267** (1995) 1924.
- [5] W. H. Zachariasen: *J. Am. Chem. Soc.* **54** (1932) 3841.
- [6] K.-H. Sun: *J. Am. Ceram. Soc.* **30** (1947) 277.
- [7] A. Zeidler *et al.*: *Phys. Rev. Lett.* **113** (2014) 135501.
- [8] Y. Onodera *et al.*: *NPG Asia Mater.* **12** (2020) 85.
- [9] H. Hashimoto *et al.*: *Sci. Rep.* **12** (2022) 516.
- [10] C. Koyama *et al.*: *NPG Asia Mater.* **12** (2020) 43.
- [11] S. Kohara *et al.*: *Nat. Commun.* **5** (2014) 5892.